Preprints (www.preprints.org) | NOT PEER-REVIEWED | Posted: 4 May 2023 doi:10.20944/preprints202305.0267.v1

Disclaimer/Publisher's Note: The statements, opinions, and data contained in all publications are solely those of the individual author(s) and contributor(s) and not of MDPI and/or the editor(s). MDPI and/or the editor(s) disclaim responsibility for any injury to people or property resulting from any ideas, methods, instructions, or products referred to in the content.

Article

Investigation of Electrochromic, Combinatorial TiO_2-SnO_2 Mixed Layers by Spectroscopic Ellipsometry using Different Optical Models

Noor Taha Ismaeel[1,2,5] [0000-0002-0087-4766], Zoltán Lábadi[1], Peter Petrik[1,4], Miklós Fried[1,3*]

[1]Institute of Technical Physics & Materials Science, Centre for Energy Research, Konkoly-Thege Rd. 29-33, Budapest 1121, Hungary
[2]Doctoral School on Materials Sciences and Technologies, Óbuda University, Budapest, Hungary
[3]Institute of Microelectronics and Technology, Óbuda University, Tavaszmezo Str. 17, Budapest 1084, Hungary
[4]Department of Electrical Engineering, Institute of Physics, Faculty of Science and Technology, University of Debrecen, 4032 Debrecen, Hungary
[5]Institute of Laser for Postgraduate Studies, University of Baghdad, Iraq; noor.t@ilps.uobaghdad.edu.iq
* fried.miklos@uni-obuda.hu.

Abstract: We determined the optimal composition of reactive magnetron sputtered TiO_2-SnO_2 mixed layers for electrochromic purposes. We determined and mapped the composition and optical parameters by Spectroscopic Ellipsometry (SE). The Ti- and Sn- targets have been placed separately, and the Si-wafers on glass substrate (30 cm× 30 cm) were moved under the two separated targets (Ti and Sn) in Ar-O_2 plasma. Different (Effective Medium Approximation (EMA) and oscillator-type) optical models were used to obtain the composition maps and thickness of the sample layer. Scanning Electron Microscopy (SEM) with Energy-Dispersive X-ray Spectroscopy (EDS) has been used to check the SE results. The 'goodness' of diverse optical models have been compared, according to the conditions of sample preparation. We show that in the case of molecular-level mixed layers 2-Tauc-Lorentz oscillator model is better than the Bruggeman Effective Medium Approximation (BEMA). The electrochromic properties of mixed metal oxides that deposited by reactive sputtering have been mapped, too.

Keywords: Titanium-Tin Oxide; reactive sputtering; spectroscopic ellipsometry; electrochromic materials

1. Introduction

Metal oxides are widely studied with respect to their electrochromic behavior and properties for the applications as display devices and smart windows. To decrease the absorbed heat in buildings, electrochromic films have been used as smart windows for preservation the glass windows from the extra heating [1]. Electrochromic materials have been applied in energy-effective vitrification, automobile sunroofs, smart windows, and mirrors. Transition metal oxides such as titanium, tungsten, nickel, vanadium, and molybdenum oxides have been considered the most promising electrochromic materials [2]. The formation of smart window contains a layer of electrochromic material bounded by metal oxide layers. To turn transparent glass opaque and back to the transparent state, low electric current is used. The transmittance can be controlled by modifying the optical properties.

The protection from heat radiation through glass is made by semiconductor metal oxide film coatings on glass, such as TiO_2, WO_3, CrO, NiO, Nb_2O_5, and IrO_2 [3], MoO_3 [4, 5]. Typically, nanoscale oxides are considered according to their high thermal conductivity, low thermal expansion coefficient and the insulation. Application of this type of coating gives advanced surface quality. The heat transfer rate and the thermal conductivity have been increased due to the increases in concentration of nano particles. [6, 7].

© 2023 by the author(s). Distributed under a Creative Commons CC BY license.

Preprints (www.preprints.org) | NOT PEER-REVIEWED | Posted: 4 May 2023 doi:10.20944/preprints202305.0267.v1

Several methods of deposition can be considered: sputtering [8], sol-gel method [4], sintering [9], Atmospheric Pressure Chemical Vapor Deposition (APCVD) [10], and dipping [11].

The colored state of pure TiO_2 coatings is gray and this oxide was not used alone in electrochromic devices because its coloration is not very strong [3]. Titanium oxide films have been sputter-deposited in a non-aqueous medium, spray deposited from reactive sputtering. Chronoamperometric experiments associated with transmittance spectra in $LiClO_4$-propylene carbonate solutions were carried out and compared with the optical properties of titanium oxide films with different stoichiometries. [12].

Spectroscopic Ellipsometry (SE) is a high accuracy optical characterization technique [13]. Many researchers have used SE for pure or combinatorial material investigation [14-21].

Combinatorial approach to investigate mixed metal oxides has several advantages. Fried et al. [22] have used SE (which is fast, cost-effective, and non-destructive method) for investigation and mapping WO_3-MoO_3 mixed layers after sputtering. Different optical models (such as Effective Medium Approximation (EMA) and oscillator-type ones) have been used to achieve the composition map and thickness map of the sample layers.

While TiO_2 was investigated as electrochromic material [23], SnO_2 or TiO_2-SnO_2 [24, 25] mixtures were studied only as photocatalytic materials. During this work, reactive magnetron sputtering (in Ar-O_2 plasma) has been used to produce all combinations of TiO_2-SnO_2 mixed layers on silicon wafers. The sample preparation time took 4 hours in the vacuum chamber including the vacuum-preparation time. By using the combinatorial process, all the compositions have been achieved in the same sputtering chamber after one sputtering. Scanning Electron Microscopy (SEM) with Energy-Dispersive X-ray Spectroscopy (EDS) has been used to check the SE results.

The object of this work was to investigate the goodness of TiO_2-SnO_2 mixed layers as electrochromic materials, and to contrast the 'goodness' of the diverse optical models, and to enhance the electrochromic properties demeanor of mixed metal oxides that were deposited by reactive sputtering. We expected that using different diameter metal atoms in the layer will have a positive effect.

2. Materials and Methods

In the chamber of magnetron sputtering, the layers were deposited in a reactive (Ar + O_2) gas mixture in ~2×10^{-6} mbar high vacuum, was the pressure of the process was ~10^{-3} mbar. 30 sccm/s Ar and 30 sccm/s O_2 volumetric flow rate has been applied inside the chamber. The substrates were 4-inch diameter IC-grade and 3-inch diameter highly conductive (0.001 Ωcm) Si-wafers.

The movement speed was 5 cm/s (back and forth) in the geometry which can be seen in Fig. 1. 50-50 % composition can be expected in the middle of the specimen. The Si-wafers and control Si-stripes were placed on a 30 cm × 30 cm glass, see Fig.1. The power of the plasma was in the range of 0.75–1.5 kW for the two targets, and independently controlled. 300 walking cycles were applied with 5 cm/s movement speed.

Figure 1 presents that sputtering targets have been placed at 35 cm from each other. According to the measurements, the two sputtered material fluxes 'material streams' are overlapped around the center. The Metal/Oxygen atomic ratio in the layers was 1:2 at the applied Oxygen partial pressure according to the SEM-EDS analysis technique.

Preprints (www.preprints.org) | NOT PEER-REVIEWED | Posted: 4 May 2023 doi:10.20944/preprints202305.0267.v1

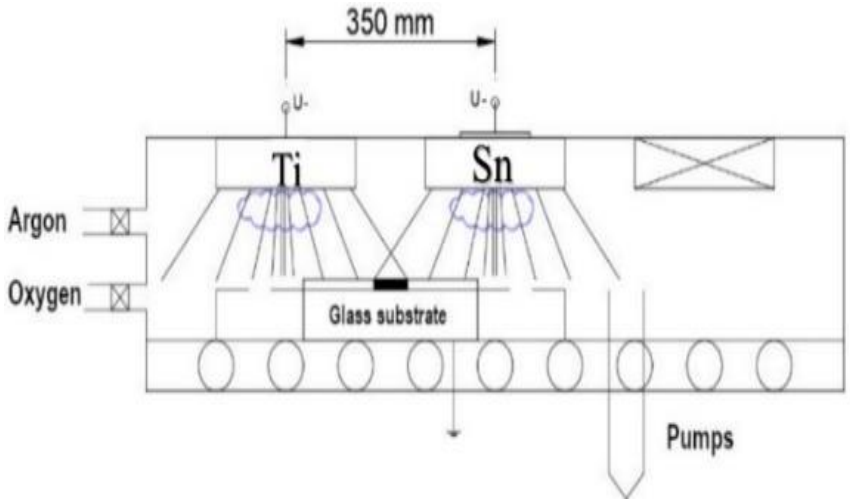

Figure 1. Arrangements of the two targets in closer position (35 cm from each other).

The optical mapping [21] was performed by a Woollam M2000 SE equipment, the measurements were evaluated with the CompleteEASE software [26]. To obtain the mapping parameters, oscillator functions and compact optical models have been used. The „goodness" of the optical model depends on the value of the Mean Squared Error (MSE), so the lower MSE refers to the better fit because of the difference between curves. [13] The silicon wafers and Si-stripes (Fig. 2 (a) have been used for Scanning Electron Microscopy (SEM, Dual-beam SEM+FIB Thermo Scientific Scios2) with Energy Dispersive Spectroscopy (EDS) measurements, too, see Fig. 2 (b). The Ti/Sn ratio has been calculated point-by-point to compare and validate the results of the SE evaluation.

(a) **(b)**

Figure 2. (a) Graded TiO_2-SnO_2-layer-on-3 inch-Si (circular sample, upper) and the Si-stripe samples, lower; **(b)** Combinatorial TiO_2-SnO_2 layer on a 4-inch Si-wafer in the SEM-chamber (Dual-beam SEM+FIB Thermo Scientific Scios2).

The coloration process was followed point by point of the layer deposited onto the 3-inch diameter highly conductive (0.001 Ωcm) Si-wafer. Electrochemical measurements were performed in a liquid cell filled with 1M lithium perchlorate ($LiClO_4$) / propylene carbonate electrolyte, and a Pt wire counter electrode was placed into the electrolyte alongside with a reference electrode, see Fig. 3. Controlled current was applied through the cell during a 4 min coloration.

Preprints (www.preprints.org) | NOT PEER-REVIEWED | Posted: 4 May 2023 doi:10.20944/preprints202305.0267.v1

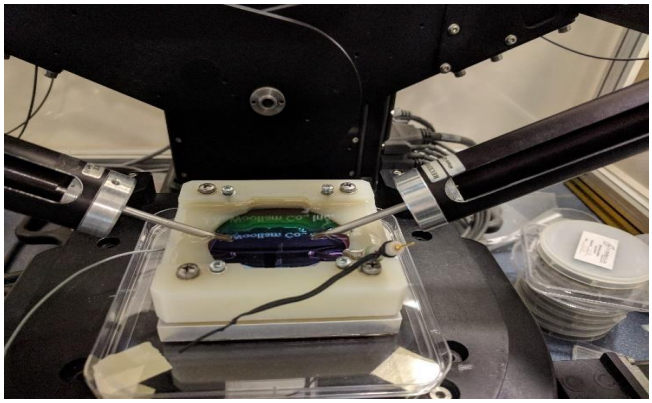

Figure 3. Combinatorial TiO_2-SnO_2 layer on highly conductive 3-inch Si-wafer in an electrochemical fluid cell during in-situ, real-time SE measurements.

After the coloration process, the whole sample (in dry state) was mapped by SE. The edges were under the Teflon cover (during the coloration process) so only the central 4 cm diameter part is interesting, see Fig. 3.

3. Results

We compared two dispersion relations in our multilayer optical model (Si-substrate/interface-layer/T-L(TiO_2)+T-L(SnO_2)-mixed layer/surface-roughness-layer). In the Bruggeman Effective Medium Approximation (EMA or BEMA [27]) calculation, the mixed-layer is considered as a physical combination of two distinct phases formed by TiO_2 and SnO_2 with an appropriate volume fraction. The constituents are considered equivalent; neither of the components is considered as a host material.The formula as in equations (1):

$$0 = \sum f_i(\varepsilon_i-\varepsilon)/(\varepsilon_i+2\varepsilon), \quad (1)$$

where ε is the effective complex dielectric function of the composite layer; f_i and ε_i denote volume fraction and the complex dielectric function of the ith component. In the case of two components, the formula is a complex quadratic equation, where ε (the effective dielectric function) is the unknown and we can choose easily between the two solutions (the wrong one is physically meaningless). The dielectric function of the two constituents were determined from the extreme edges of the Si-stripes where the TiO_2 and SnO_2 are in pure format.

The Tauc-Lorentz (T-L) oscillator model is a combination of the Tauc and Lorentz models [28]. Tauc-Lorentz (T-L) oscillator model contains four parameters: Transition Amplitude, Broadening coefficient of the Lorentz oscillator, peak position for the Lorentz oscillator, and Bandgap Energy (E_g), which is taken to be the photon energy, where ε_2 (E) reaches zero. When the E photon energy is less than the bandgap energy, E_g, ε_2 (E) is zero. The real part of the dielectric function ε_1 (E) can be obtained from ε_2 (E) through the Kramers-Kronig relation.

In the mixed layers, five fitting parameters have been used: two Amplitudes for each materials (oscillator strengths) and the layer thickness. We used the measurements near the edges of the samples (pure component materials) to determine the fundamental parameters (Bandgap Energies, the Broadenings and the Peak positions) for the two materials.

For the electrochromic measurements, where the light absorption was interesting in the visible wavelength region over 400 nm, we used the simple Cauchy formula to describe the complex refractive as in formula: N = n + ik, where N is the complex refractive index, n is the real part of N, k is the imaginary part (extinction), i is the imaginary unit. Cauchy formula: $n(\lambda) = A+B/\lambda^2+C/\lambda^4$, $k(\lambda) = ke^{U(1239.84/\lambda - Eb),}$ where A, B, C, k, and U are fitting parameters. The complex refractive index (N) and complex dielectric function (ε) are equivalents: $(\varepsilon) = \varepsilon_1+i\varepsilon_2 = N^2$, $\varepsilon_1 = n^2-k^2$, $\varepsilon_2 = 2nk$.

Preprints (www.preprints.org) | NOT PEER-REVIEWED | Posted: 4 May 2023 doi:10.20944/preprints202305.0267.v1

3.2. Comparison of the optical models

We applied the 2-T-L and the EMA optical model to evaluate the mapping measurements on the Si-stripes (see Fig. 4) and the 4-inch Si-wafer (see Fig. 5). Both modelling process gave good results, see Fig. 4 where the measured Psi and Delta spectra are in good agreement with the Model calculations. However, one can see that the MSE (Mean Squared Error) is significantly lower for the 2-T-L model especially around the 50-50 % composition, see Fig. 4 (c) and Fig. 5 lower row. The calculated thickness values are not different significantly, see Fig. 4 (d) and Fig. 5 middle row.

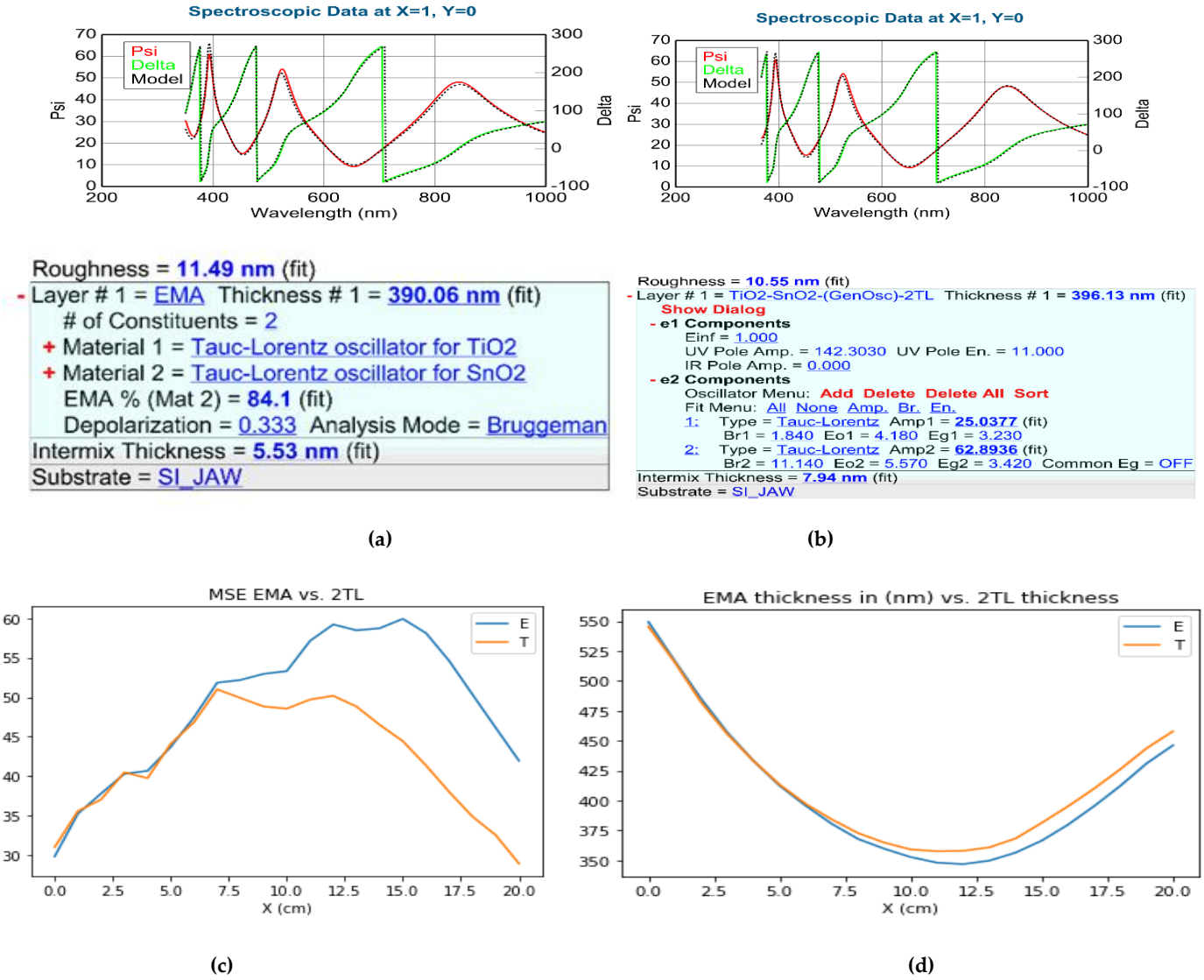

Figure 4. Comparison of **(a)** EMA; **(b)** 2T-L modelling (TiO_2-SnO_2)**; [(c)** MSE for EMA (the blue curve) vs. 2T-L (the orange curve), **(d)** is the thickness (EMA (the blue curve) vs. 2T-L (the orange curve)**]** by home-made Python software.

Preprints (www.preprints.org) | NOT PEER-REVIEWED | Posted: 4 May 2023 doi:10.20944/preprints202305.0267.v1

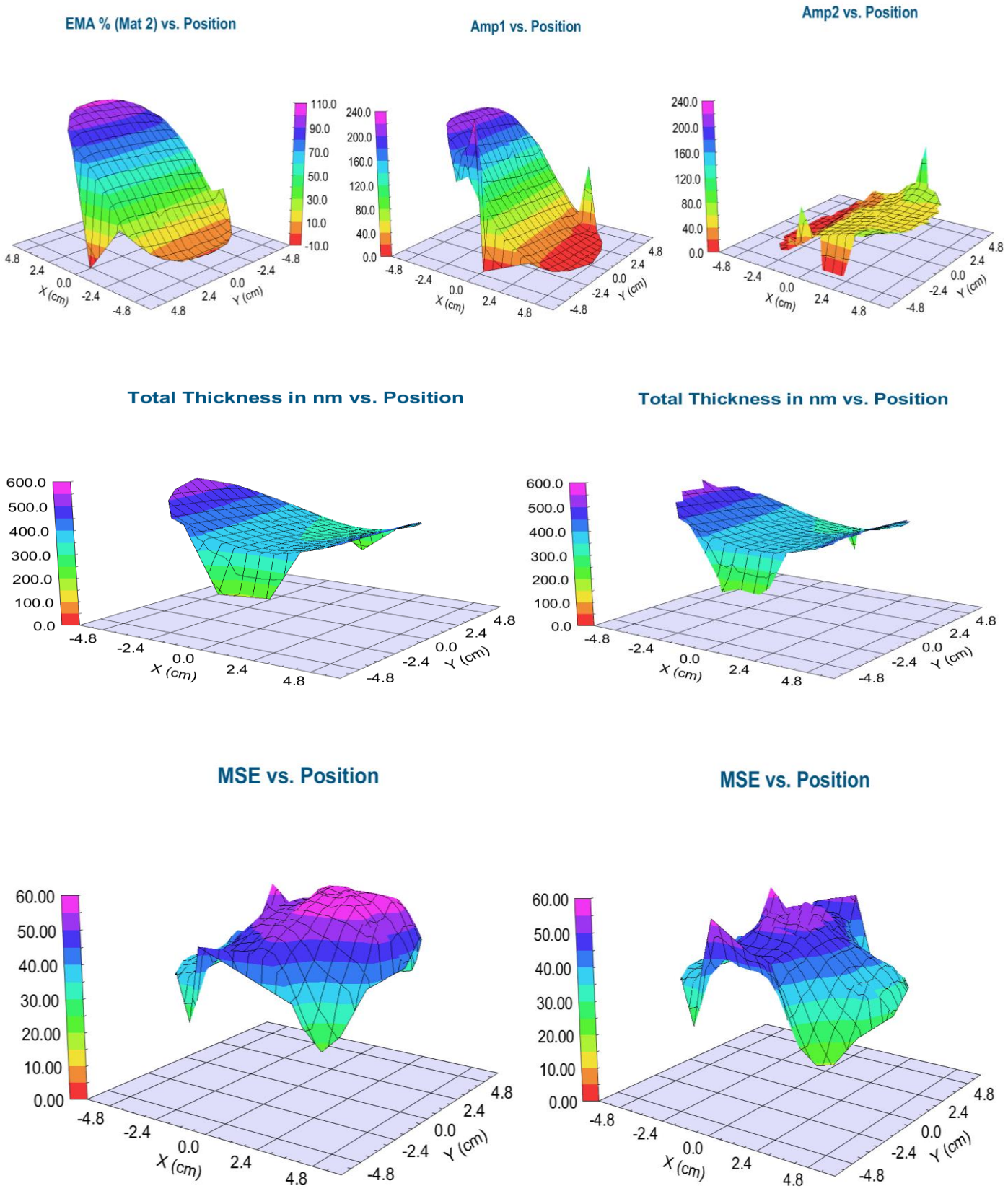

Figure 5. TiO_2-SnO_2 maps from the 4 inch-wafer by EMA modelling (left) 2T-L modelling (right), upper row: EMA% (left) and Tauc-Lorentz amplitudes (right), middle row: total thickness maps, lower row: MSE maps (showing that the 2-T-L model is better).

Preprints (www.preprints.org) | NOT PEER-REVIEWED | Posted: 4 May 2023 doi:10.20944/preprints202305.0267.v1

4. Discussion

We validated the results of the SE modeling by SEM-EDS measurements, see Fig. 6 (b). Fig. 6 (a) shows the EMA % (MAT2 - SnO_2 %) values from the EMA model and the Amp1 (TiO_2 oscillator strength) and the Amp2 (SnO_2 oscillator strength) from the 2-Tauc-Lorentz (2-T-L) model. Fig. 6 (c) shows the results together, where we normalized the Amp1 and Amp2 to 100 %. One can see the good agreement between the SEM-EDS and the 2-T-L results.

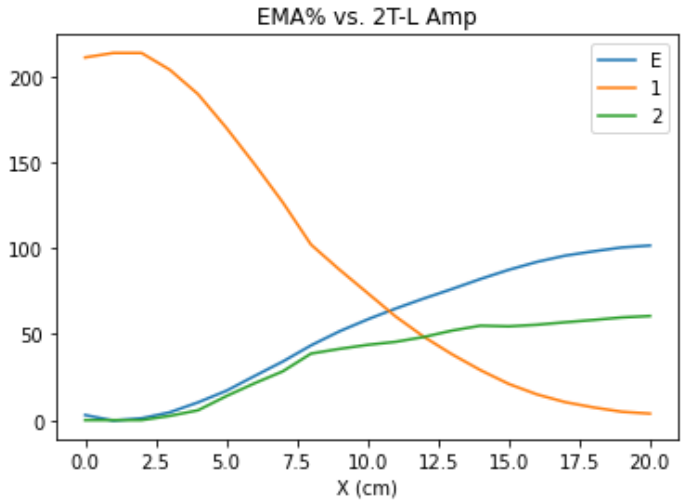

(a)

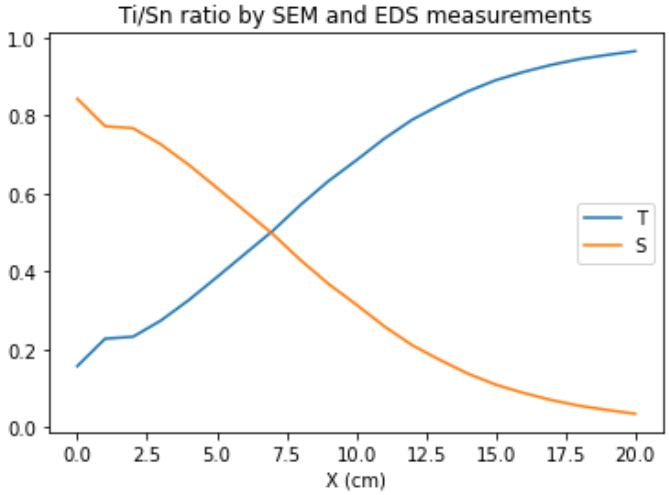

(b)

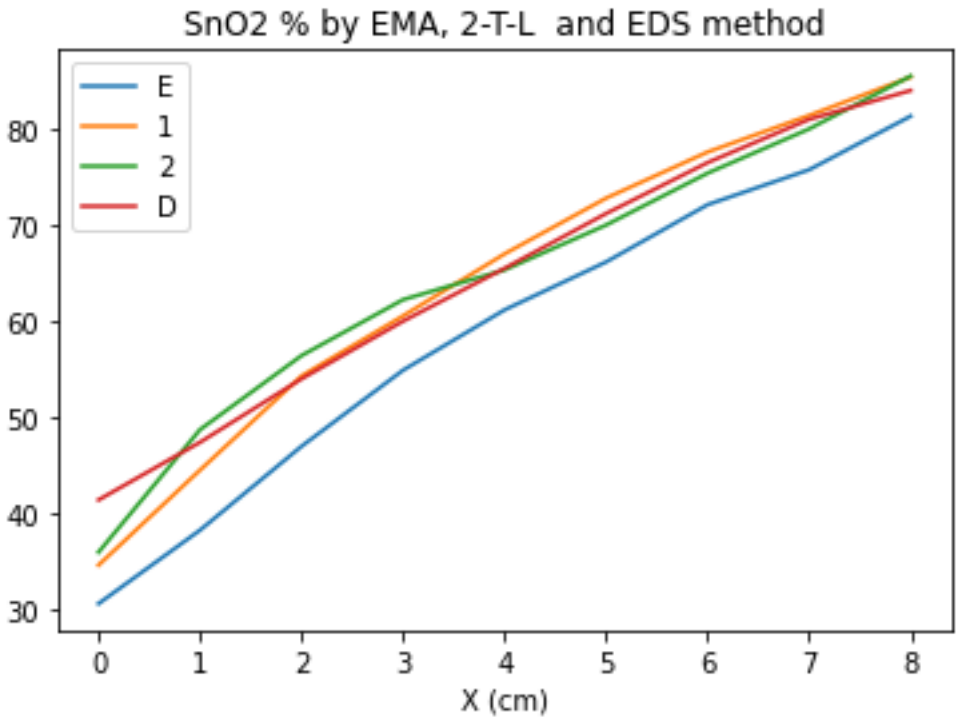

(c)

Figure 6. TiO_2-SnO_2 -4inch-ref-EMA-2TL; [(a) the blue curve for EMA %, the orange curve for Amp1 (TiO_2), the green curve for Amp2 (SnO_2)]; (b) Ti/Sn ratio by SEM and EDS measurements, (the blue curve for Ti ratio and the orange curve for Sn ratio); (c) SnO_2 % derived from EMA % (the blue

Preprints (www.preprints.org) | NOT PEER-REVIEWED | Posted: 4 May 2023 doi:10.20944/preprints202305.0267.v1

curve), 2-T-L models (the orange curve for Amp1 and the green curve for Amp2), the red curve for EDS % measurements] by home-made Python software.

4.1. Electrochromic measurements

After the validation of the SE method (we can determine the composition of the layer) we performed in-situ electrochromic measurement, see Fig. 3. We could measure only at the central point of the highly conductive 3-inch Si-wafer. Fig. 7 show a typical example of one measured spectra pair with the Model calculation based on the Optical model shown on the right side. Low MSE value shows that the optical model is good. We could follow the process, calculating the change of the k parameter, see Fig. 8 (a).

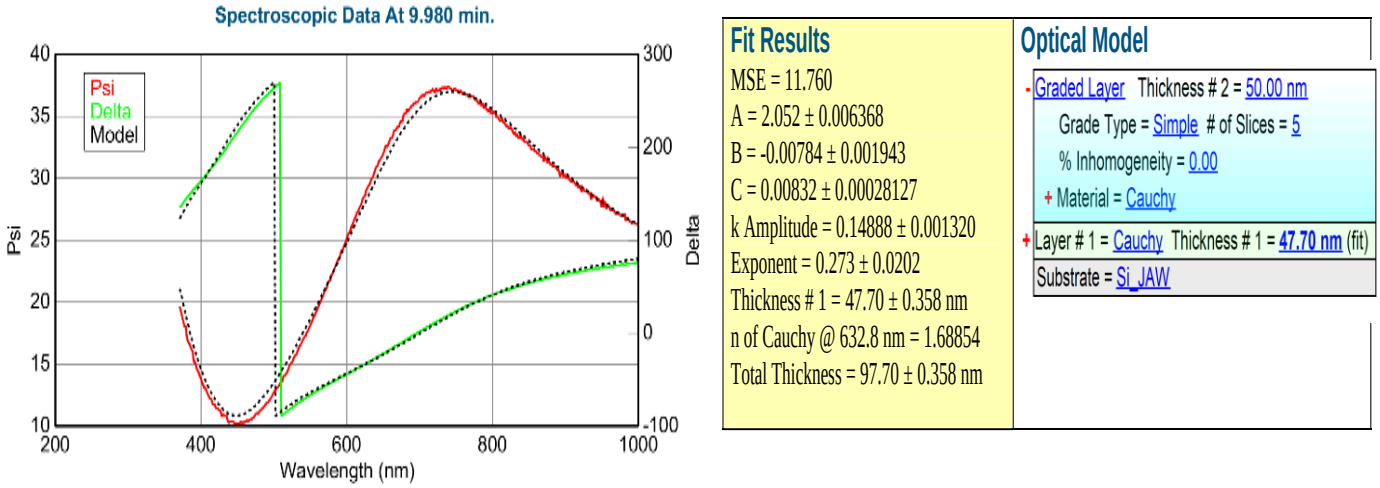

Figure 7. Shows a typical example of a fitted SE spectrum for the details of the model structure; SE spectra were evaluated using a multi-layer; multi-parameter optical model applying graded Cauchy-dispersion.

After the coloration process, we could map the colorized layer using a simple one-layer Cauchy dispersion optical model. (Note, that this is not the same model as it was used in the in-situ measurement!) We see a maximum value (maximum light absorption) around 0.5 cm. Comparing this results with Fig. 6, we can state that the optimal composition is at $TiO_{2\ 0,3}$-$SnO_{2\ 0,7}$.

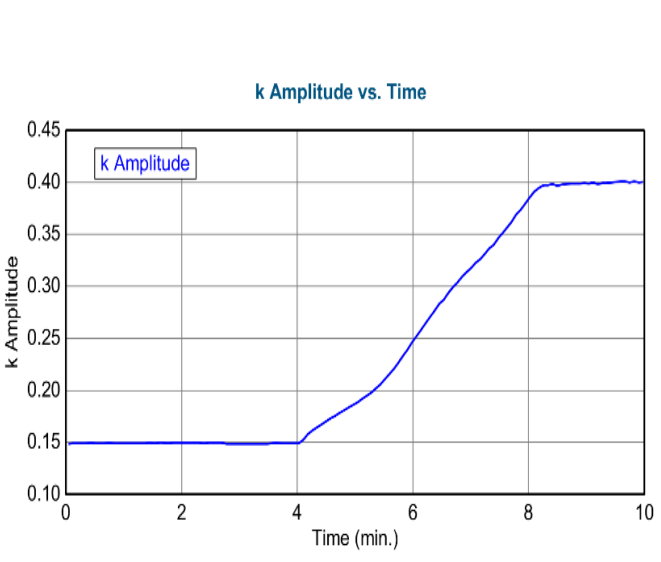

(a)

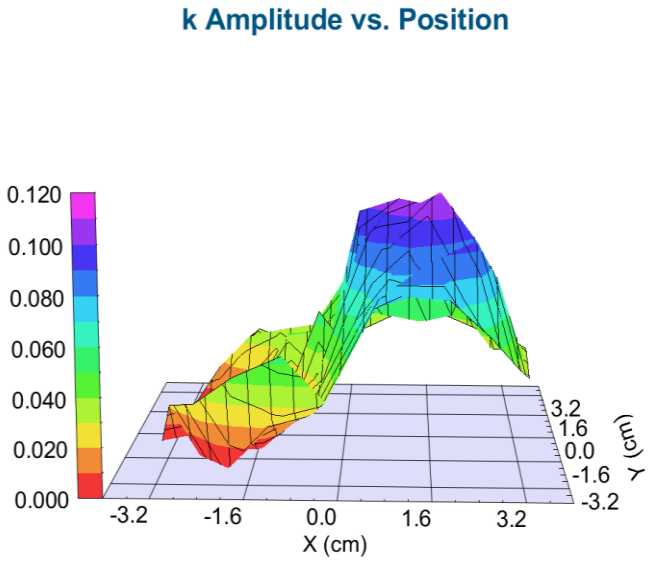

(b)

Preprints (www.preprints.org) | NOT PEER-REVIEWED | Posted: 4 May 2023 doi:10.20944/preprints202305.0267.v1

Figure 8. **(a)** Imaginary part of the Refractive index (k Amplitude) as a function of time for highly-conductive-Si in liquid-cell during coloration (time-scan, simple Cauchy-model), here we can mention that from (0-4) minute's there is low absorption but from (4-8) minute's there is a growing absorption; **(b)** Map of the k parameter after coloration (simple Cauchy-model).

5. Conclusions

We could optimize the electrochromic properties of mixed metal oxides deposited by reactive sputtering. We prepared combinatorial samples by magnetron sputtering. These samples have been mapped (composition and thickness maps) by Spectroscopic Ellipsometry which is a fast, cost-effective, and non-destructive method. We can select between suitable optical models (the Bruggeman Effective Medium Approximation, BEMA vs. 2-Tauc-Lorentz oscillator model) according upon the process parameters. We have shown that in case of molecular-level mixed layers 2-Tauc-Lorentz oscillator model is better than the Bruggeman Effective Medium Approximation. We have shown that the optimal composition is at. $TiO_{2\ 0,3}$-$SnO_{2\ 0,7}$.

Acknowledgments: This research was funded by NKFIH OTKA NN 131269 (VOC-DETECT M-ERA.NET Transnational Call 2018) and NKFIH OTKA K 128319 and 131515 projects. Project TKP2021-EGA-04 has been implemented with the support provided by the Ministry of Innovation and Technology of Hungary from the National Research, Development, and Innovation Fund, financed under the TKP2021 funding scheme. The work in frame of the 20FUN02 ''POLight'' project has received funding from the EMPIR programme co-financed by the Participating States and from the European Union's Horizon 2020 research and innovation programme. Noor Taha Ismaeel is grateful for the Stipendium Hungaricum scholarship.

References

1. Granqvist, C.G. Handbook of Inorganic Electrochromic Materials. *Elsevier*, Amsterdam, The Netherlands **1995**.
2. Yingxi Lu; Liang Liu; Daniel Mandlerb and Pooi See Lee. High switching speed and coloration efficiency of titanium-doped vanadium oxide thin film electrochromic devices. *Journal of Materials Chemistry C*. October **2013**, DOI: 10.1039/C3TC31508H.
3. Livage, J.; Ganguli, D. Sol-gel electrochromic coatings and devices. A review. *Sol. Energy Mater. Sol. Cells* **2001**, pp. 365–381.
4. Lin, S.-Y.; Wang, C.-M.; Kao, K.-S.; Chen, Y.-C.; Liu, C.-C. Electrochromic properties of MoO_3 thin films derived by a sol–gel process. *J. Sol Gel Sci. Technol* **2010,** pp. 53, 51–58.
5. Hsu, C.S.; Chan, C.C.; Huang, H.T.; Peng, C.H.; Hsu, W.C. Electrochromic properties of nanocrystalline MoO_3 thin films. *Thin Solid Film* **2008**, pp. 516, 4839–4844.
6. M. I. Kandil; H. S. Jahin; et al. Synthesis and characterization of γ- Al_2O_3 and α-Al_2O_3 nanoparticles using a facile, inexpensive autocombustion approach. *Egypt. J. Chem.* **2021**, Volume 64, No.5, pp. 2509 – 2515.
7. Kusammanavar Basavaraj; Dr. K Elangovan; Dr. Suneelkumar N Kulkarni; Dr. Shankar S. Effect of Concentration of Al_2O_3 Nano Particles in Base Fluid on Thermal and Flow Properties to Enhance the Heat Transfer Rate. *INTERNATIONAL JOURNAL OF ENGINEERING RESEARCH & TECHNOLOGY (IJERT)* **2021**, Volume 10, Issue 02.
8. Madhavi, V.; Jeevan Kumar, P.; Kondaiah, P.; Hussain, O.M.; Uthanna, S. Effect of molybdenum doping on the electrochromic properties of tungsten oxide thin films by RF magnetron sputtering. *Ionics* **2014**, pp. 20, 1737–1745.
9. Prameelaand, C.; Srinivasarao, K. Characterization of $(MoO_3)_x$-$(Wo_3)_{1-x}$ composites. *International Journal of Applied Engineering Research* **2015**, pp.10, 9865–9875.
10. Ivanova, T.; Gesheva, K.A.; Kalitzova, M.; Hamelmann, F.; Luekermann, F.; Heinzmann, U. Electrochromic mixed films based on WO_3 and MoO_3 obtained by an APCVD method. *J. Optoelectron. Adv. Mater* **2009**, pp. 11, 1513–1516.
11. Novinrooz, A.; Sharbatdaran, M.; Noorkojouri, H. Structural and optical properties of WO_3 electrochromic layers prepared by the sol-gel method. *Cent. Eur. Sci. J.* **2005**, pp. 3, 456–466.
12. M.P. Cant; J.I. Cisnero; R.M. Torresib. Electrochromic behavior of sputtered titanium oxide thin films. *ELSEVIER, Thin Solid Films* **1995**, pp. 259, 70-74.
13. Hiroyuki Fujiwara. *Spectroscopic Ellipsometry Principles and Applications*, Publisher: John Wiley & Sons, 2007; ISBN: 0470060182, 9780470060186.
14. Zimmer, A.; Gilliot, M.; Broch, L.; Boulanger, C.; Stein, N.; Horwat, D. Morphological and chemical dynamics upon electrochemical cyclic sodiation of electrochromic tungsten oxide coatings extracted by in situ ellipsometry. *Appl. Opt.* **2020**, pp. 59,3766–3772.
15. Hales, J.S.; DeVries, M.; Dworak, B.; Woollam, J.A. Visible and infrared optical constants of electrochromic materials for emissivity modulation applications. *Thin Solid Film* **1998**, pp.313–314, 205.
16. Sauvet, K.; Rougier, A.; Sauques, L. Electrochromic WO_3 thin films active in the IR region. *Sol. Energy Mater. Sol. Cells* **2008**, pp. 92, 209–215.

Preprints (www.preprints.org) | NOT PEER-REVIEWED | Posted: 4 May 2023 doi:10.20944/preprints202305.0267.v1

17. Shan, A.; Fried, M.; Juhasz, G.; Major, C.; Polgár, O.; Németh, Á.; Petrik, P.; Dahal, L.R.; Chen, J.; Huang, Z. High-speed imaging/mapping spectroscopic ellipsometry for in-line analysis of roll-to-roll thin-film photovoltaics. *IEEE J. Photovolt* **2014**, pp. 4, 355–361.
18. Koirala, P.; Tan, X.; Li, J.; Podraza, N.J.; Marsillac, S.; Rockett, A.; Collins, R.W. Mapping spectroscopic ellipsometry of CdTe solar cells for property-performance correlations. In Proceedings of the 2014 IEEE 40th Photovoltaic Specialist Conference (PVSC), Denver, CO, USA, pp. 0674–0679, 8–13 June (2014).
19. Dahal, L.R.; Li, J.; Stoke, J.A.; Huang, Z.; Shan, A.; Ferlauto, A.S.; Wronski, C.R.; Collins, R.W.; Podraza, N.J. Applications of real-time and mapping spectroscopic ellipsometry for process development and optimization in hydrogenated silicon thin-film photovoltaics technology. *Sol. Energy Mater. Sol. Cells* **2014**, pp. 129, 32–56.
20. Aryal, P.; Pradhan, P.; Attygalle, D.; Ibdah, A.-R.; Aryal, K.; Ranjan, V.; Marsillac, S.; Podraza, N.J.; Collins, R.W. Real-time, in-line, and mapping spectroscopic ellipsometry for applications in Cu (in Ga) Se metrology. *IEEE J. Photovolt* **2014**, pp. 4, 333–339.
21. Peter Petrik; Miklos Fried. Mapping and Imaging of Thin Films on Large Surfaces. A review. *physica status solidi (a)* **2022**, Volume 219, 2100800, https://doi.org/10.1002/pssa.202100800. Published by Wiley-VCH GmbH381.
22. Fried, M.; Bogar, R.; Takacs, D.; Labadi, Z.; Horvath, Z.E.; Zolnai, Z. Investigation of Combinatorial WO_3-MoO_3 Mixed Layers by Spectroscopic Ellipsometry Using Different Optical Models. *Nanomaterials* **2022**, pp. 12, 2421. https://doi.org/10.3390/nano12142421.
23. Erbil Şilik; Suat Pat; Soner Özen; Reza Mohammadigharehbagh; H. Hakan Yudar; Caner Musaoğlu; Şadan Korkmaz. Electrochromic properties of TiO_2 thin films grown by thermionic vacuum arc method. *Thin Solid Films* **2017**, Volume 640, pp. 27-32, https://doi.org/10.1016/j.tsf.2017.07.073.
24. Shankar Sharma; Naveen Kumar; Peter R. Makgwane; Nar Singh Chauhan; Kavitha Kumari; Manju Rani; Sanjeev Maken. TiO_2/SnO_2 nano-composite: New insights in synthetic, structural, optical and photocatalytic aspects, *Inorganica Chimica Acta* **2022**, Volume 529, 120640, https://doi.org/10.1016/j.ica.2021.120640.
25. Rekha B. Rajput; Shweta N. Jamble; Rohidas B. Kale. A review on TiO_2/SnO_2 heterostructures as a photocatalyst for the degradation of dyes and organic pollutants. *Journal of Environmental Management* **2022**, Volume 307, 114533, https://doi.org/10.1016/j.jenvman.2022.114533.
26. Available online: https://www.jawoollam.com/products/m-2000-ellipsometer (accessed on 2022-07-12).
27. Bruggeman, D.A.G. Dielectric constant and conductivity of mixtures of isotropic materials. *Ann. Phys.* **1935**, Volume 24, pp. 636–664. https://doi.org/10.1002/andp.19354160705.
28. Jellison, G.E., Jr.; Modine, F.A. Parameterization of the optical functions of amorphous materials in the inter band region. *Appl. Phys. Lett.* **1996**, Volume 69, pp. 371–373.